Biophysical characterization of the SARS-CoV-2 E protein

Authors

Aujan Mehregan (1), Sergio Pérez-Conesa (2), Yuxuan Zhuang (3), Ahmad Elbahnsi (2), Diletta Pasini (1), Erik Lindahl (2,3), Rebecca J Howard (3)*, Chris Ulens (1)*, Lucie Delemotte (2)*

Affiliations

1. Laboratory of Structural Neurobiology, Department of Cellular and Molecular Medicine, Faculty of Medicine, KU Leuven, Leuven, Belgium
2. Department of Applied Physics, Science for Life Laboratory, KTH Royal Institute of Technology, Solna, Sweden
3. Department of Biochemistry and Biophysics, Science for Life Laboratory, Stockholm University, Solna, Sweden
*Corresponding authors: lucied@kth.se, chris.ulens@kuleuven.be, rebecca.howard@dbb.su.se

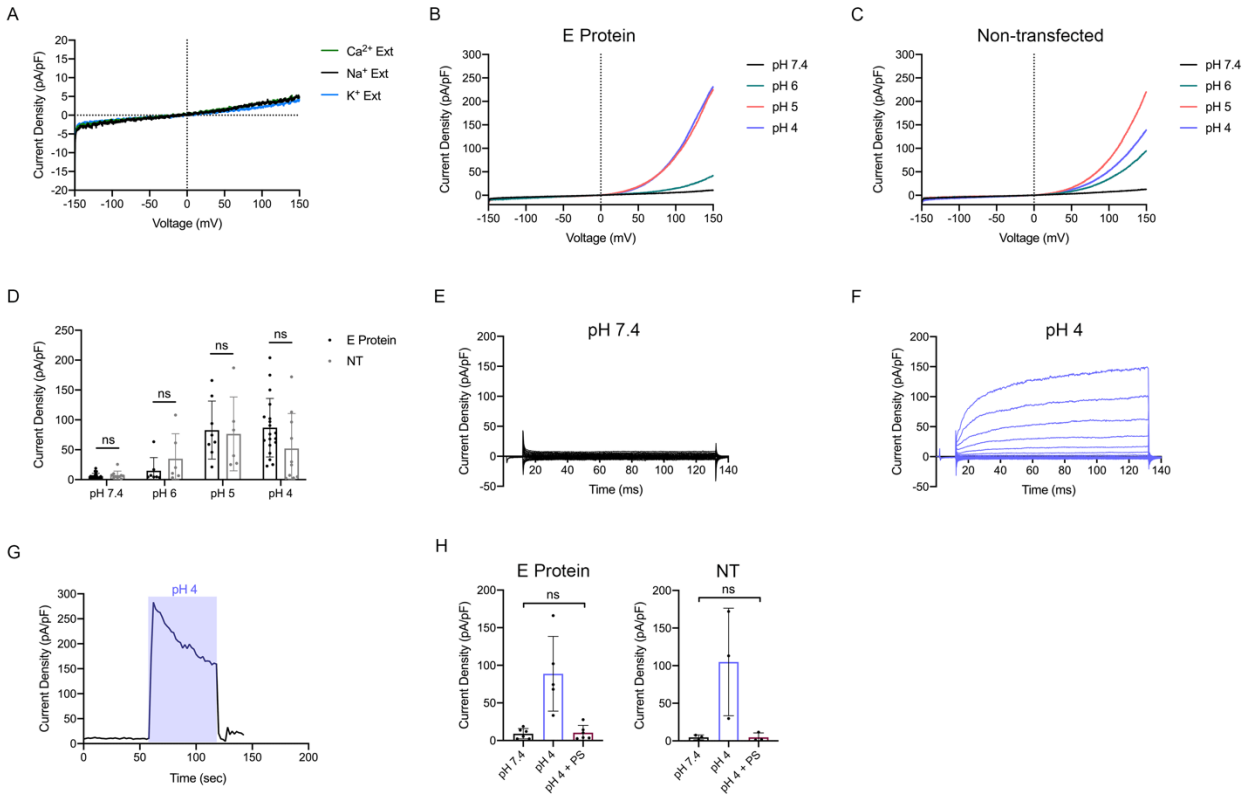

Figure S1. No evidence of activity at the plasma membrane in HEK-293 cells

Cells transiently transfected with the EcGFP construct displayed outward currents in acidic conditions, but could not be consistently distinguished from non-transfected cells. A: Representative traces of EcGFP-transfected cells perfused with modified standard extracellular solution containing only $CaCl_2$ (green trace), NaCl (black trace), or KCl (blue trace) (N = 7). B: Mean traces of EcGFP-transfected cells perfused with standard extracellular solution in decreasing pH, 1 min exposures (pH 7.4 N = 24; pH 6 N = 7; pH 5 N = 8; pH 4 N = 19). C: Mean traces of non-transfected cells under the same conditions as in A (pH 7.4 N = 10; pH 6 N = 6; pH 5 N = 6; pH 4 N = 10). D: Comparison of outward current densities analyzed at +100 mV. Statistical significance was calculated via an unpaired, non-parametric Mann-Whitney test; ns = not significant ($p > 0.05$). E-F: Current traces in response to voltage steps from -160 mV to +40 mV in 20 mV increments from EcGFP-transfected cells. E: Current response in extracellular solution of pH 7.4 vs. F: of pH 4. G: Time course illustrating on/off kinetics in response to a 1 min exposure of extracellular solution at pH 4 (blue shaded region). H: In a subset of experiments, 50 µM PS was added after switching to an extracellular solution of pH 4, resulting in a nearly complete block of outward current in response to pH. Values in this condition were statistically not significant compared to values at pH 7.4: E protein (N = 6; $p > 0.05$); NT (N = 3; $p > 0.05$); calculated using a paired, non-parametric Wilcoxon test.

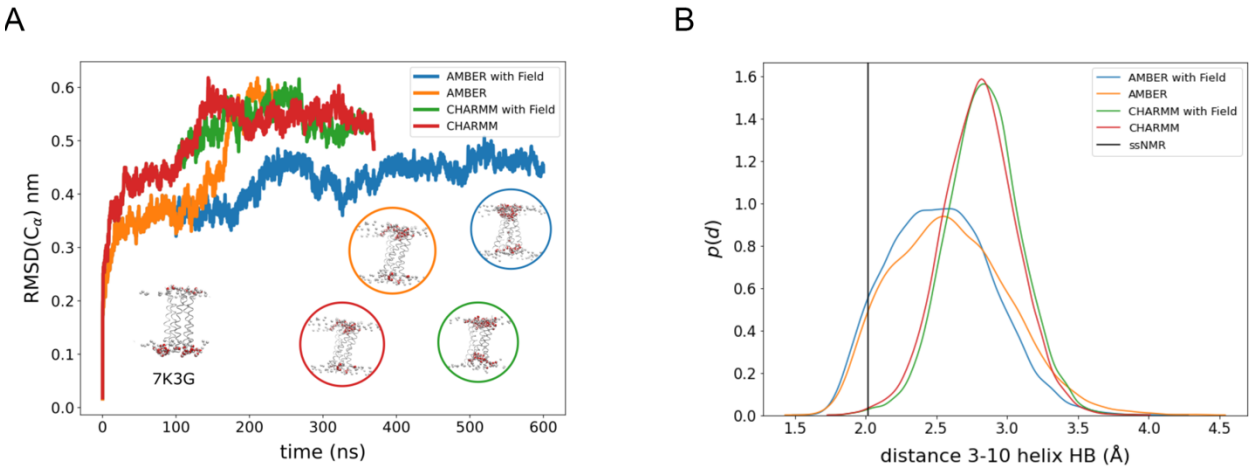

Figure S2. Limited stability of the closed solid-state NMR structure (PDB ID 7K3G)
A: Root mean-squared deviations (RMSDs) of Cα atoms as a function of time during simulations of the pentameric solid-state NMR structure (PDB ID: 7K3G). Models were simulated in the CHARMM36m (red, green) or AMBER99SB-ILDN + SLIPIDS (blue, orange) force fields in the absence (red, orange) or presence (green, blue) of an electric field. Inset snapshot at lower left shows the starting model, viewed from membrane plane; additional insets show snapshots from the end of the simulations. B: Probability distribution of the backbone hydrogen-bond distance (O of F20 to H of F23) that defines the 3_{10}-helix transition, in the four simulations colored as in *A*. The vertical black line indicates the hydrogen-bond distance in the solid-state NMR structure.

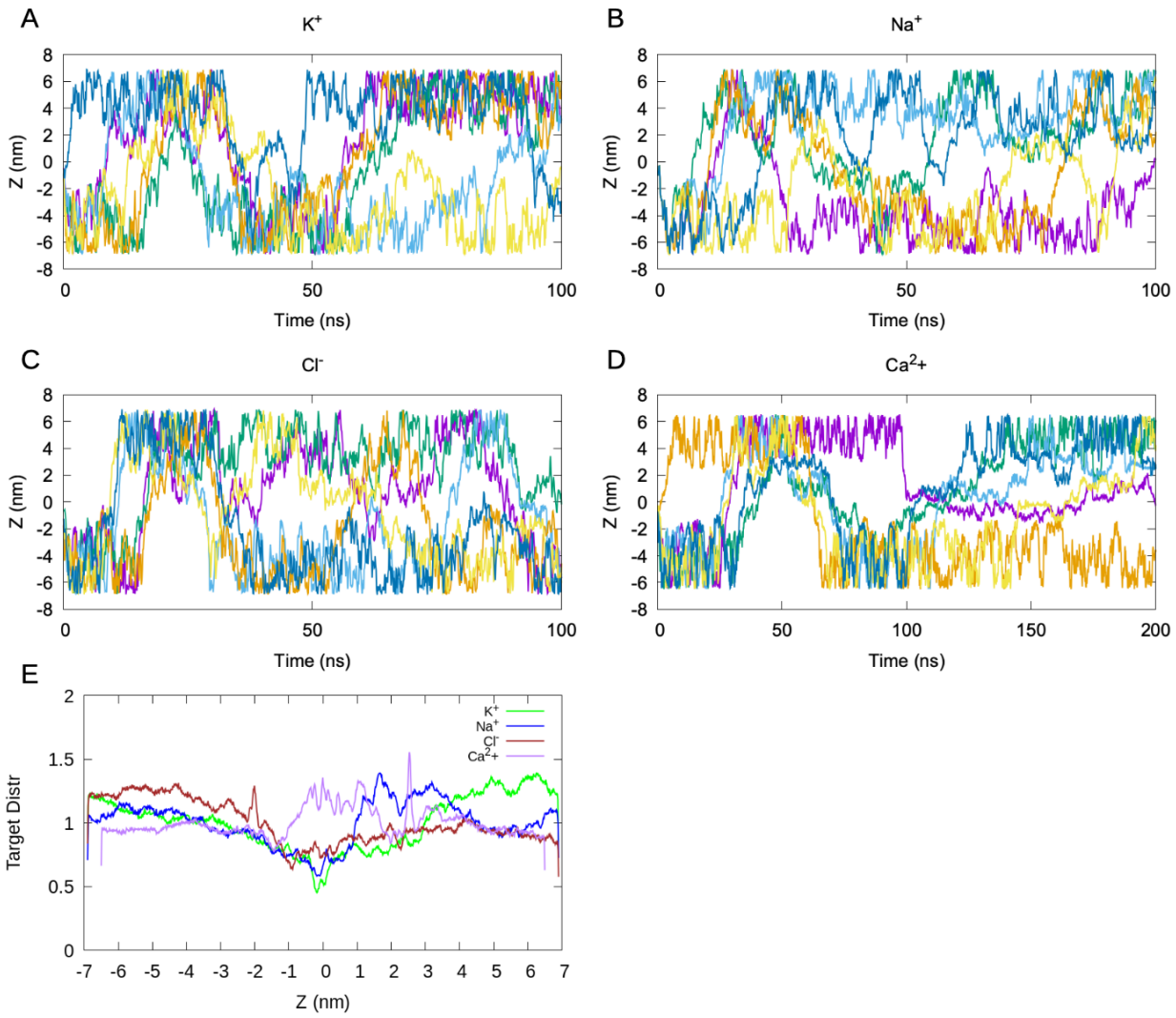

Figure S3: Convergence of ion-permeation simulations in the most stable E-protein simulation model.

Ion movement along the Z-axis of the pore as a function of time in accelerated-weight histogram simulations of permeation through the most stable E-protein simulation model by A: K+, B: Na^+, C: Cl^-, or D: Ca^{2+}. Different walkers are shown in different colors. E: Target distribution as a function of the pore Z-axis for K^+ (green), Na^+ (blue), Cl^- (red) and Ca^{2+} (purple) ion-permeation simulations.

Table S1: Atomistic MD simulations. Conditions are identified by starting structures (PDB ID and ensemble-model number; pentamerized monomers, 'x 5'; homology model based on SARS-CoV variant, 'mod.'), post-translational modifications (PTM; palmitoylated, 'palm.'; glycosylated, 'glyc.'), equilibration protocols (CHARMM-GUI default protocol, 'GUI'; with an electric field, '+ Field'; with pore restraints based on Ref. 38, '+ Pore restraints'), and production conditions (CHARMM36m force field, 'CHARMM'; AMBER99SB-ILDN + SLipids force field, 'AMBER'). Most simulations produced asymmetrized (asymm.) or collapsed endpoints, with only simulation 8 producing a possibly conductive state over hundreds of nanoseconds.

ID	Structure	PTM	Equilibration	Production	Result
1	2MM4.1 x 5, mod.	None	GUI	CHARMM	Asymm., collapsed
2	2MM4.1 x 5, mod.	None	+ Field	CHARMM + Field	Asymm., collapsed
3	2MM4.1 x 5, mod.	Palm.	+ Field	CHARMM	Asymm., collapsed
4	2MM4.1 x 5, mod.	Palm.	+ Field	CHARMM + Field	Asymm., collapsed
5	5X29.1, mod.	None	GUI	CHARMM	Asymm., collapsed
6	5X29.1, mod.	None	GUI	CHARMM	Mostly symmetric, collapsed
7	5X29.1, mod.	None	+ Pore restraints	CHARMM	Asymm., collapsed
8	5X29.1, mod.	None	+ Pore restraints	CHARMM + Field	Mostly symmetric, possibly open
9	5X29.1, mod.	None	GUI	CHARMM + Field	Mostly symmetric, collapsed
10	5X29.1, mod.	Palm.	GUI	CHARMM	Asymm., collapsed
11	5X29.1, mod.	Palm., glyc.	GUI	CHARMM	Asymm., collapsed
12	5X29.1, mod.	Glyc.	GUI	CHARMM	Asymm., collapsed
13	5X29.6, mod.	None	+ Pore restraints	CHARMM + Field	Asymm., collapsed
14	5X29.7, mod.	None	+ Pore restraints	CHARMM + Field	Asymm., collapsed
15	7K3G.1	None	+ Pore restraints	AMBER + Field	Asymm., collapsed
16	7K3G.1	None	+ Pore restraints	AMBER	Mostly symmetric, collapsed
17	7K3G.1	None	+ Pore restraints	CHARMM + Field	Mostly symmetric, collapsed
18	7K3G.1	None	+ Pore restraints	CHARMM	Mostly symmetric, collapsed